



## Accumulation of cholesterol suppresses oxidative phosphorylation and altered responses to inflammatory stimuli of macrophages

Yi-Chou Chiu<sup>a</sup>, Pei-Wen Chu<sup>b</sup>, Hua-Ching Lin<sup>c,d</sup>, Shau-Kwaun Chen<sup>b,\*</sup>

<sup>a</sup> Division of General Surgery, Surgical Department, Cheng-Hsin General Hospital, Taipei City, Taiwan

<sup>b</sup> Institute of Neuroscience, National ChengChi University, Taipei City, Taiwan

<sup>c</sup> Division of Colorectal Surgery, Surgical Department, Cheng-Hsin General Hospital, Taipei City, Taiwan

<sup>d</sup> Department of Healthcare Information and Management, Ming Chuan University, Taoyuan County, Taiwan

### ARTICLE INFO

#### Keywords:

Cholesterol  
Macrophage  
Oxidative phosphorylation  
Oxidative stress  
Inflammatory response

### ABSTRACT

Hypercholesterolemia induces intracellular accumulation of cholesterol in macrophages and other immune cells, causing immunological dysfunctions. On cellular levels, cholesterol enrichment might lead to mitochondrial metabolic reprogramming and change macrophage functions. Additionally, as cholesterol is permeable to the plasma membrane and might integrate into the membranous organelles, such as endoplasmic reticulum or mitochondria, cholesterol enrichment might change the functions or properties of these organelles, and ultimately alters the cellular functions. In this study, we investigate the mitochondrial alterations and intracellular oxidative stress induced by accumulation of cholesterol in the macrophages, and the possible immunological impacts caused by these alterations. Macrophage cells RAW264.7 were treated with cholesterol to induce intracellular accumulation of cholesterol, which further triggered the reduced production of reactive oxygen/nitrogen species, as well as decrease of oxidative phosphorylation. Basal respiration rate, ATP production and non-mitochondrial oxygen consumption are all suppressed. In contrast, glycolysis remained unaltered in this cholesterol-enriched condition. Previous studies demonstrated that metabolic profiles are associated with macrophage polarization. We further verified whether this metabolic reprogramming influences the macrophage responses to pro-inflammatory or anti-inflammatory stimuli. Our results showed the changes of transcriptional regulations in both pro-inflammatory and anti-inflammatory genes, but not specific toward M1 or M2 polarization. Collectively, the accumulation of cholesterol induced mitochondrial metabolic reprogramming and suppressed the production of oxidative stress, and induced the alterations of macrophage functions.

### 1. Introduction

In recent years, cellular metabolism has been identified as a key regulator of macrophage function by influencing signal transduction and gene regulation [1,2]. Metabolic reprogramming of mitochondria in myeloid cells is associated with both inflammatory and anti-inflammatory responses [3,4]. For example, upregulation of glycolysis facilitates the macrophage activation and cytokine production (M1 state), while oxidative phosphorylation induces alternative activation of macrophages (M2 state) [5]. Unbalanced lipid metabolism also leads to a series of cellular alterations in macrophage and is associated with various pathological events [6]. Most of the studies related to this topic have been focused on the role of cholesterol-laden macrophages in atherosclerosis. Hypercholesterolemia leads to the accumulation of free

cholesterol in macrophage and alterations of macrophage properties [7, 8]. In atherosclerotic artery, increased levels of oxidized low-density lipoprotein (LDL) triggers macrophage mediated scavenging. Modified LDL functions as a ligand for macrophage pattern recognition receptors, including Toll-like receptors (TLRs), and can directly activate pro-inflammatory signaling pathways. In addition, LDL engulfed by macrophages, caused intracellular cholesterol accumulation, which also amplifies TLR signaling, and in turn increased production of cytokines and chemokines with amplification of the downstream inflammatory process [9,10]. Accumulation of cholesterol stimulates intracellular formation of cholesterol crystals, which interacts biochemically with the inflammasome component NLRP3 to influence inflammasome activity and IL-1 $\beta$  production [11,12]. In addition to the upregulation on inflammatory signaling and the production of inflammatory mediators,

\* Corresponding author. Institute of Neuroscience, National ChengChi University, No. 64, Sec. 2, Zhinan Rd., Wenshan Dist., Taipei City, 11605, Taiwan, ROC.  
E-mail address: [chensk@nccu.edu.tw](mailto:chensk@nccu.edu.tw) (S.-K. Chen).

<https://doi.org/10.1016/j.bbrep.2021.101166>

Received 1 August 2021; Received in revised form 26 October 2021; Accepted 28 October 2021

2405-5808/© 2021 The Authors. Published by Elsevier B.V. This is an open access article under the CC BY-NC-ND license

(<http://creativecommons.org/licenses/by-nc-nd/4.0/>).

other impacts of cholesterol accumulation on macrophage properties and functions have not been fully characterized.

The accumulation of intracellular cholesterol also leads to the change of the properties and functions of membranous organelles, and in turn affect macrophage functions [13,14]. Cholesterol is one of the major structural constituents of the plasma membrane and membranous organelles, functioning to maintain the integrity and fluidity [15]. Although cholesterol levels in mitochondria are lower than in the plasma membrane, and in the endoplasmic reticulum (ER), the low levels of cholesterol might make mitochondrial membranes highly sensitive to even small changes in their absolute cholesterol content. Loading with cholesterol results in mitochondrial alterations in a variety of cell types. In hepatocytes, enrichment of cholesterol impairs oxidative phosphorylation and disrupts the assembly of respiratory complex [16]. The effects of cholesterol enrichment on oxidative stress might be cell type-dependent. The decrease of oxidative phosphorylation reduces the production of oxidative stress. On the other hand, compromised membrane fluidity by cholesterol integration decreases 2-oxoglutarate carrier activity [17], which leads to reduced  $\alpha$ -ketoglutarate transport and impaired glutathione (GSH) import into mitochondria, possibly causing the elevation of oxidative stress. Increase of cholesterol contents also leads to the alterations of membrane permeability and ultimately influencing cell viability. In macrophages, accumulation of intracellular cholesterol results in the concentration-dependent diversification in cell viability [18]. This apoptotic event has been linked to the formation of foam cell and pathogenesis of atherosclerosis [10]. Mitochondrial dysfunctions in the cholesterol-enriched conditions have been reported in several pathophysiological conditions, such as several types of cancers, myocardial ischemia and hepatosteatosis [19]. However, the mitochondrial functions, as well as the properties and functions of non-apoptotic macrophages in hypercholesterolemia have not been determined. Mitochondria play pivotal roles in various macrophage functions, including activation, polarization, and the formation of NLRP3 inflammasome [20]. Thus, the mitochondrial functions might be altered in cholesterol-laden macrophage and consequently influence the immunological functions.

Here we investigated the impacts of accumulated free cholesterol on mitochondrial functions in non-apoptotic macrophages. ROS/RNS levels and oxidative phosphorylation in the macrophage treated with excessive cholesterol were examined. Also, macrophage functions, including activation and polarization with M1 or M2 stimulation, were also elucidated. We reported that mitochondria functions and production of oxidative stress both decreased in cholesterol-loaded macrophages. Additionally, accumulation of cholesterol appeared to alter the macrophage responses to pro-inflammatory and anti-inflammatory stimuli in a gene-dependent manner, possibly due to the change he membrane fluidity alters various signaling pathways. The changes are not specific to either M1 or M2 polarization.

## 2. Materials and methods

**Cells and materials.** The murine macrophage cell line RAW264.7 subclone 2 was obtained from ATCC (ATCC® TIB-71™). Cells were grown in DMEM (Gibco; Thermo Fisher Scientific, Inc.) supplemented with 10% (v/v) FBS, 1% (v/v) penicillin-streptomycin solution, and incubated at 37 °C in 5% CO<sub>2</sub> humidified air. Water-soluble cholesterol (cholesterol-methyl- $\beta$ -cyclodextrin) was purchased from Sigma-Aldrich (C4951). The hydrophobic cholesterol is conjugated with hydrophilic methyl- $\beta$ -cyclodextrin, which makes the cholesterol molecules aggregates in the core when dissolved in aqueous conditions such as in culture medium, and is commonly used for the loading of the cholesterol in the cultured cells [18,21]. In the study, RAW264.7 cells were incubated with or without water-soluble cholesterol at a final concentration of 20  $\mu$ g/ml cholesterol-methyl- $\beta$ -cyclodextrin.

**Filipin staining and immunocytochemistry.** RAW264.7 cells were fixed for 15min with 4% paraformaldehyde and permeabilized with

0.1% Triton X-100 in 1xPBS for 10min, and then blocked with 2% bovine serum albumin (BSA). Anti-Prohibitin (GeneTex, GTX101105: 1:200) primary antibody was incubated overnight, followed by a secondary antibody for 1 h. After the incubation of secondary antibody, Filipin III (Cayman 70440) was added at 0.05 mg/ml and incubated for 2 h. Stained samples were mounted with ProLong Gold Antifade Mountant (ThermoFisher P10144). The images were pictured with a Zeiss AxioImager A1 microscope.

**Flow Cytometry.** The raw cells were cultured in a six-well plate at an appropriate condition. The cells were treated with cholesterol for 24 h after the cells grew to an appropriate density. The raw cells were collected and then analyzed with a CytoFLEX flow cytometer (Beckman Coulter, Inc., Brea, California, USA). Data were analyzed using the CytExpert Software.

**In vitro ROS/RNS detection.** OxiSelect™ In vitro ROS/RNS assay kit (green fluorescence) (Cell Biolabs, cat. STA-347) was used to measure ROS and RNS in macrophage cell line RAW264.7. Cells were homogenized and centrifuged at 10,000 g for 5 min to remove insoluble particles. 50  $\mu$ l of supernatant was mixed with 50  $\mu$ l catalyst (provided in the kit) to accelerate the oxidative reaction. Following 5 min incubation at room temperature, 100  $\mu$ l DCFH-DiOxyQ probe solution was added to the mixture to measure the total free radical population. The DCFH probe can react with free radical molecules that are representative of both ROS and RNS. The samples were incubated at room temperature for 30 min and read with a fluorescence plate reader at excitation/emission = 480/530 nm. The standard curve of H<sub>2</sub>O<sub>2</sub> was used to quantify the free radical content in the cell lysates.

**Seahorse Oxygen Consumption Rate (OCR) And Mitochondrial Stress Test.** The raw cells were plated at  $2.5 \times 10^4$  cells per well in 24-well Seahorse V7 culture plates (Agilent Seahorse catalog # 100777-004) in the appropriate medium. Cells were treated with cholesterol for 24 h, subsequently, measured OCR on a Seahorse XFe24 as described by the manufacturer (Agilent Technologies), with some modifications. After the treatment, cells were changed into DMEM with no additional exogenous substrates, and additions were made through the injection ports: for the mitochondrial stress test, respectively, the following concentrations of the inhibitors were used: 1  $\mu$ M oligomycin, 0.5  $\mu$ M FCCP and 0.5  $\mu$ M each of antimycin A and rotenone. Wave software was used to determine oxygen consumption.

**Reverse transcription quantitative PCR (RT-qPCR) assay.** Total RNA was extracted using RNAzol® reagent (Mrcgene; Molecular research center, Inc.), according to the manufacturer's protocol. cDNA was synthesized using a IQ2 MMLV RT-Script kit (Bio-Genesis Technologies Inc.) according to manufacturer's protocol. qPCR was performed using SYBR-Green (Applied Biosystems, Thermo Fisher Scientific, Inc.), and data collection was conducted using an ABI 7300 (Applied Biosystems; Thermo Fisher Scientific, Inc.). The PCR cycling conditions were as follows: 95 °C for 2 min, followed by 40 cycles at 95 °C for 20 s, 56 °C or 53 °C for 20 s and 72 °C for 40 s, a final extension step of 95 °C for 15 s, 60 °C for 1 min, 95 °C for 15 s and 60 °C for 15 s. Glyceraldehyde 3-phosphate dehydrogenase (GAPDH) was used as an internal control for normalization. Gene expression was calculated using the delta-delta Ct method. Primer sequences were as follow:

GAPDH:

Forward: GCACAGTCAAGGCCGAGAAT

Reverse: GCCTTCTCCATGGTGGTAA;

Bad:

Forward: CTCCGAAGGATGAGCGATGAG

Reverse: TTGTGCGATCTGTGTTGCAGT;

Bax:

Forward: TGAAGACAGGGCCCTTTTGG

Reverse: AATTCGCCGGAGACACTCG;

UCP1:

Forward: AGGCTTCCAGTACCATTAGGT

Reverse: CTGAGTGAGGCAAAGCTGATTT;

TNF- $\alpha$ :

Forward: CCCTCACACTCAGATCATCTTCT

Reverse: GCTACGACGTGGGCTACAG;

NOS2:

Forward: CTTTGCCACGGACGAGAC

Reverse: TCATTGTACTCTGAGGGCTGA;

Arg1:

Forward: GAATCTGCATGGGCAACC

Reverse: GAATCCTGGTACATCTGGGAAC;

Ym1:

Forward: AAGAACACTGAGCTAAAACTCTCT

Reverse: GAGACCATGGCACYGAACG.

**MitoTracker green stain and image analysis.** MitoTracker Green FM (Invitrogen, USA, Cat No. M7514) was used to visualize mitochondria. After incubation with MitoTracker (40 nM diluted in culture medium, 30 min, 37 °C), the cells were washed three times with culture medium. Live cell imaging was monitored by DeltaVision imaging system (PersonalDV; GE Healthcare) using an inverted epifluorescence microscope (IX-71; Olympus) with a charge-coupled device camera (CoolSNAP ES2; Photometrics). Photographs were taken independently by using constant camera exposure settings. The level of cellular fluorescence from fluorescence microscope images and the length of the mitochondria were determined by ImageJ (This method was contributed by Luke Hammond, QBI, The University of Queensland, Australia). Please see the website (<https://theolb.readthedocs.io/en/latest/imaging/measuring-cell-fluorescence-using-imagej.html>) for the details. The formula to calculate the corrected total cell fluorescence (CTCF) is  $CTCF = \text{Integrated Density} - (\text{Area of selected cell} \times \text{Mean fluorescence of background readings})$ .

**Statistical analysis.** All data are presented as the means  $\pm$  standard error and are representative of experiments conducted in triplicate. Statistical analyses were performed using GraphPad Prism 9 software (GraphPad Software, Inc., La Jolla, CA, USA). Student t-test was used to compare data from the control and treatment groups. Symbols were considered to indicate a statistically significant difference (\* where  $p < 0.05$ , \*\* where  $p < 0.002$ , \*\*\* where  $p < 0.0002$ , \*\*\*\* where  $p < 0.0001$ ).

### 3. Results

**Incubation with free cholesterol caused structural alterations in macrophages.** Immortalized mouse macrophage cells RAW246.7 exhibited similar phenotype and responses to microbial ligands that bind to either Toll-like receptors 2, 3, and 4 to that of primary bone marrow-derived macrophages [22], thus utilized in this study to examine the macrophage properties and functions. Previous studies reported that cell viability and inflammatory phenotypes triggered by the cholesterol enriched environment were concentration-dependent and time-dependent in macrophages [18]. We first setup a treatment condition to generate viable cholesterol-loaded macrophage. Several different concentration and incubation time were tested. After comparing the cell viability and structural changes, 20  $\mu\text{g/ml}$  free cholesterol incubation for 24 h was selected. High concentration and long-term exposure of cholesterol triggers the transcriptional upregulation of pro-apoptotic genes, such as Bax and Bad, and lead to apoptosis of the macrophages [23]. We further examined the expression of Bad and Bax to assure that the treatment does not trigger apoptosis. The pro-apoptotic genes were not transcriptionally upregulated after the exposure to cholesterol (Fig. 1A). Also, no obvious cell death can be detected in the culture. The cell size and intracellular contents were determined by flow cytometry. The signals detected from forward scatter and side scatter channels represent the cell size and the intracellular structures, such as density of intracellular granules, respectively. As shown in Fig. 1B, the side scatter signals of cholesterol-loaded macrophage upshifted, showing that the incubation with cholesterol had led to structural changes in macrophage. We further examined the integration of cholesterol into mitochondria by labeling the cholesterol

and mitochondria with filipin and prohibitin, respectively (Fig. 1C). Filipin staining demonstrated that the uptaken cholesterol accumulated and scattered throughout the cytoplasm, not only located on mitochondria. The filipin signals were overlapped with prohibitin staining, indicating the accumulation of cholesterol in the mitochondria. Whether mitochondria were altered after cholesterol exposure was determined by staining the cells with MitoTracker. Mitochondrial mass, which is represented by corrected total cell fluorescence (CTCF), and morphology were evaluated by Image J software. Mitochondrial mass of each cell was increased, while mitochondria also more aggregated (Fig. 1D and E). No significant changes of the length of the cholesterol-loaded mitochondrial could be detected (Fig. 1F).

**Accumulation of cholesterol triggered mitochondrial metabolic reprogramming in the macrophages.** Mitochondrial functions of cholesterol loaded macrophages were evaluated with the mitochondrial stress test by Seahorse XFe24 Analyzer. Fig. 2 illustrated the results from cholesterol-loaded macrophage and non-treated control. 24-hour exposure to free cholesterol compromised basal oxygen consumption rate (OCR) ( $p = 0.0169$ ), but not extracellular acidification (ECAR) of macrophages, (Fig. 2A and B), meaning that mitochondrial respiration was suppressed, whereas glycolysis remained unaltered. The ratio of ECAR/OCR were decreased, suggesting that cholesterol accumulation induces metabolic reprogramming. The application of electron transport chain drugs revealed significantly impaired mitochondrial respiration, including basal respiration ( $p = 0.0369$ ), ATP production ( $p = 0.0269$ ) in cholesterol enriched macrophages (Fig. 2C). Other mitochondrial features, including the maximum respiration, spare respiratory capacity and coupling efficiency all maintained at a constant level, indicating the mitochondrial structure, flexibility and function were kept undisrupted (Fig. 2C). The unchanged proton leak also suggested that no major damages were made to mitochondrial membranes after the exposure of cholesterol. In summary, accumulation of cholesterol did not generate major damages on mitochondria, but triggered metabolic reprogramming by inhibiting mitochondrial respiration and oxidative phosphorylation.

**ROS/RNS levels were decreased in cholesterol-loaded macrophage.** ROS/RNS levels in macrophage mainly come from oxidative phosphorylation, the actions of several oxidative enzymes in the cytosol, such as NADPH oxidase. The enzyme activities of those enzyme could be calculated by mitochondrial stress test as non-mitochondrial oxidative consumptions. As shown in Fig. 2, oxidative phosphorylation was suppressed by the accumulation of cholesterol. This phenomenon also supported the observation that the oxidative stress in the cholesterol loaded macrophage will be decreased (Fig. 3A). We further determined the intracellular levels of ROS/RNS in control and cholesterol loaded macrophages by a specific ROS/RNS fluorogenic probe (dichlorodihydrofluorescein DiOxyQ (DCFH-DiOxyQ)), which can detect hydrogen peroxide ( $\text{H}_2\text{O}_2$ ), peroxy radical ( $\text{ROO}^\cdot$ ), nitric oxide (NO) and peroxynitrite anion ( $\text{ONOO}^-$ ) with high sensitivity. ROS and RNS species can react with DCFH, which is rapidly oxidized to the highly fluorescent 2', 7'-dichlorodihydrofluorescein (DCF). The levels of DCF are representative of the summation of ROS and RNS. Fig. 3B demonstrated that intracellular DCF from cholesterol-loaded macrophages were significantly increased.

Mitochondrial uncoupling is another important mitochondrial event negatively regulating oxidative phosphorylation and ROS production [24]. Since mitochondrial uncoupling is mainly regulated at transcriptional levels [25], we further examined the expression levels of uncoupling genes *UCPI*. Transcriptional levels of *UCPI* was upregulated in cholesterol enriched macrophages (Fig. 3C), indicating that most of the oxidative stress generating routes and oxidative consumption were downregulated by cholesterol accumulation.

**Accumulation of cholesterol altered the response to M1 and M2 stimulus.** The metabolic profiles of macrophage have been known as important regulators of macrophage phenotypes, such as activation and polarization. Previous studies demonstrated that accumulation of

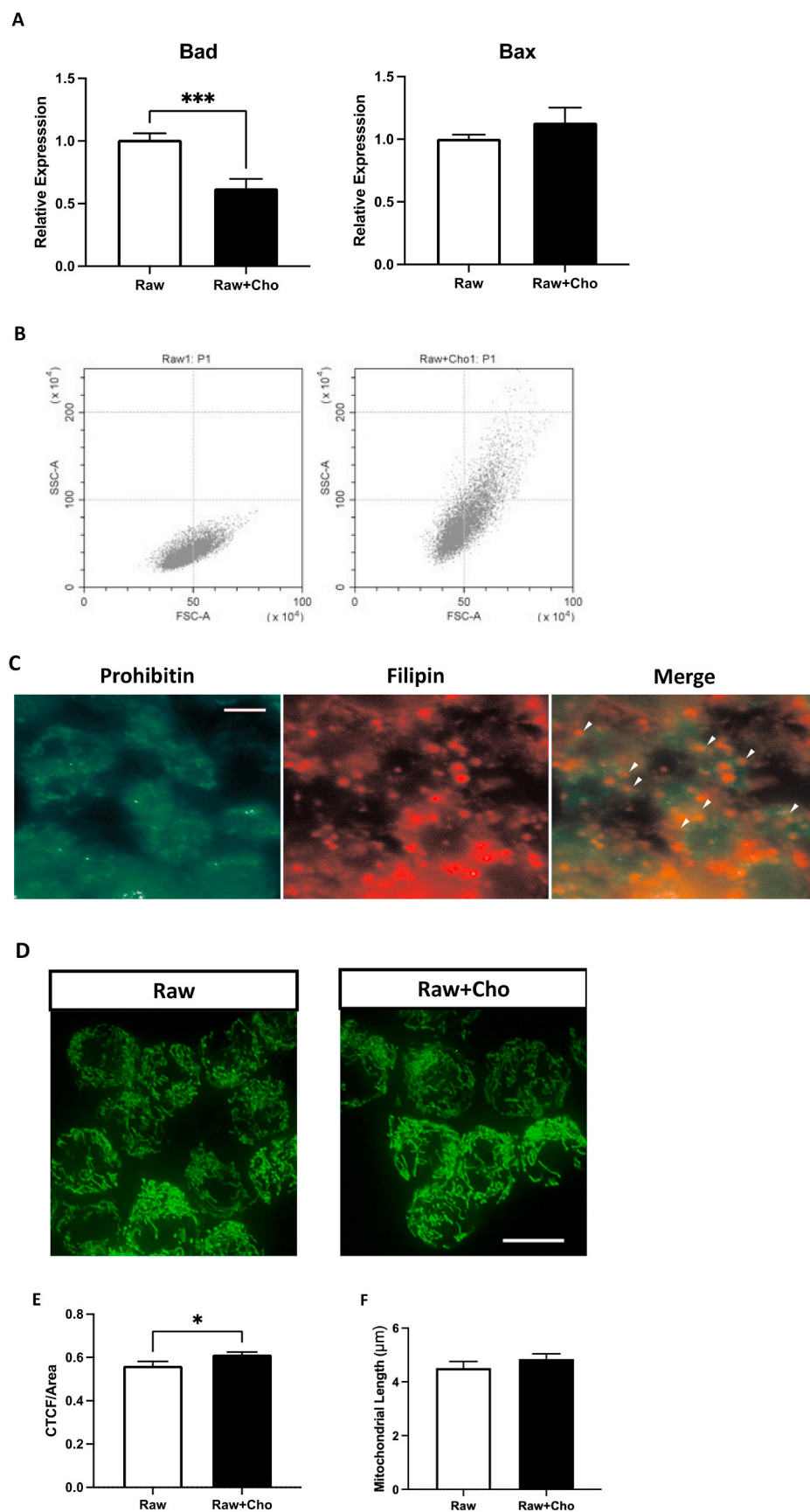


**Fig. 1. Free cholesterol induced structural alterations in macrophages.** (A) Represents the expression of apoptotic genes Bad and Bax in macrophages after cholesterol treatment. (B) Represents the cell size and intracellular contents of macrophages after the exposure to cholesterol by using the flow cytometry. (C) Indicates the loading of cholesterol on mitochondria. (D) Demonstrates the mitochondrial morphology by staining with Mito-Tracker. The white scale bar represents the 10 µm in both C and D. Results represented the mitochondrial mass/area (E) and length (F) were evaluated and analyzed with Image J software. Each column represents the mean ± SEM of at least three independent experiments. Symbols indicate significance difference between treatment and non-treatment raw cells (\* where  $p < 0.05$ , \*\*\* where  $p < 0.0002$ ).

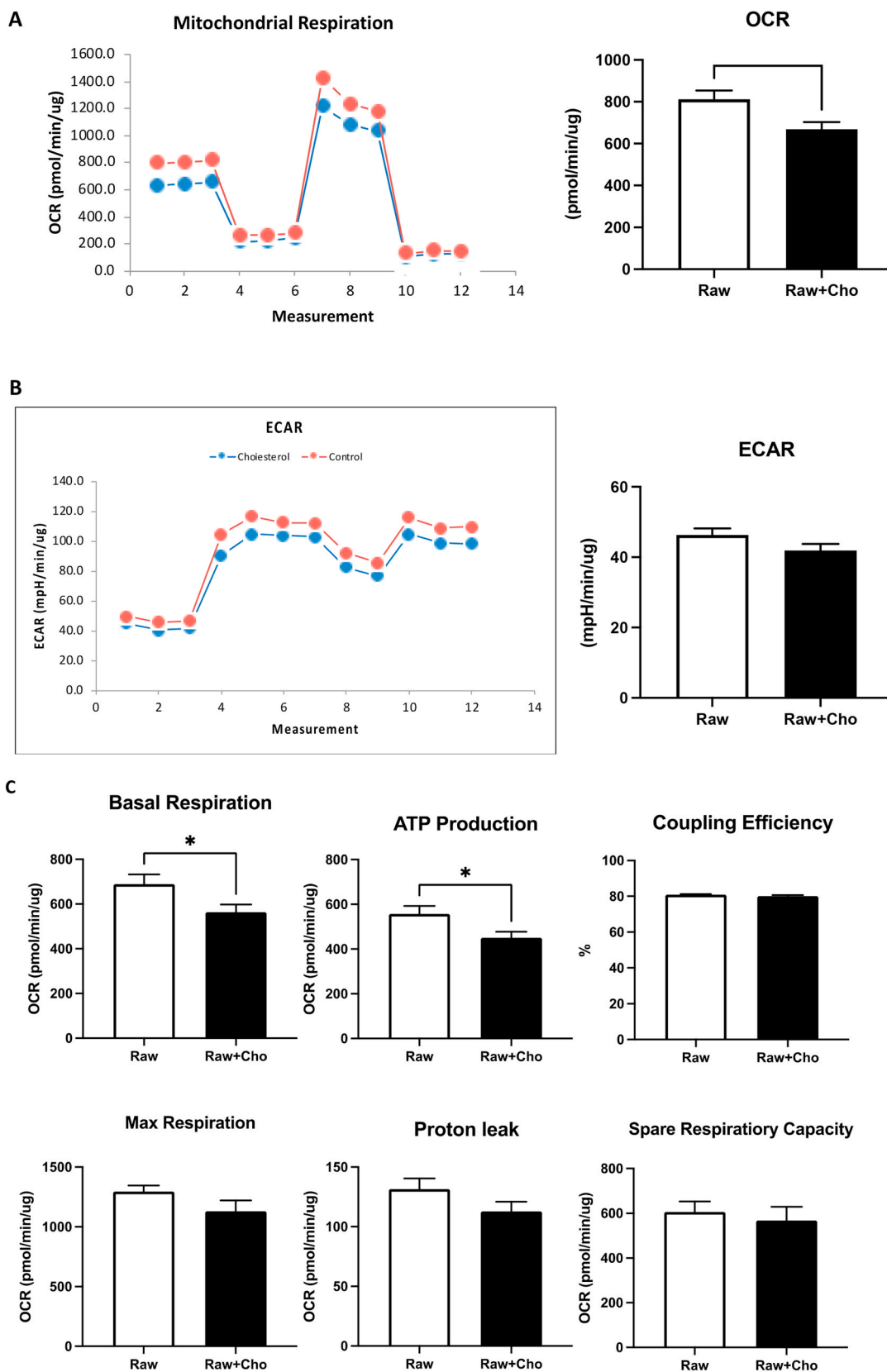


**Fig. 2. Accumulation of cholesterol altered mitochondrial functions.** (A) and (B) represents the OCR and ECAR in the macrophages separately after the exposure to cholesterol. The “Measurements” indicates the number of measurements made by Seahorse XFe24. Both the OCR and the ECAR values were automatically measured by the machine every 5.5 min. (C) The Seahorse XFe24 analyzer was employed to determine the mitochondrial function of macrophages exported to cholesterol for 24 h. Each column represents the mean ± standard error of the mean of at least three independent experiments. Symbols indicate significance difference between control group and cholesterol treated group (\* where  $p < 0.05$ ).

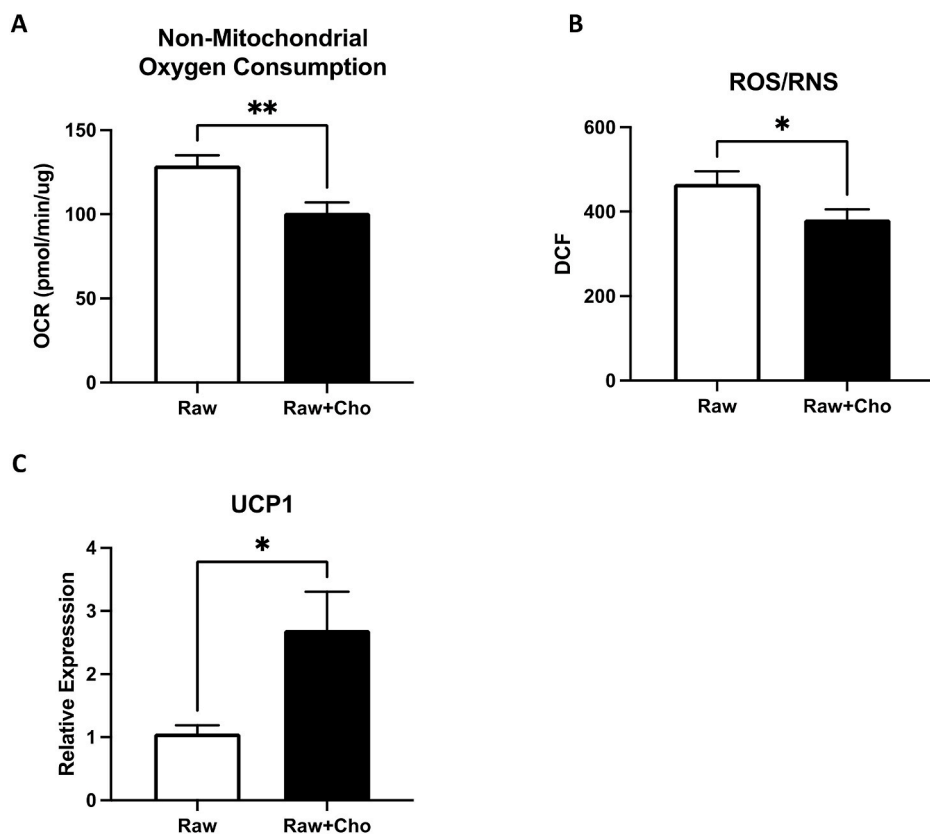


**Fig. 3. ROS/RNS levels were decreased in cholesterol-loaded macrophages.** (A) Represents the non-mitochondrial oxidative consumptions in the cholesterol loaded macrophages. (B) Quantitative levels of reactive oxygen species and reactive nitrogen species measured in macrophages after exposure to cholesterol for 24 h. (C) Quantitative levels of uncoupling genes *UCP1* expression were measured by qPCR in macrophages after exposure to cholesterol for 24 h. Each column represents the mean  $\pm$  SEM of at least three independent experiments. Symbols indicate significance difference between control group and treated group (\* where  $p < 0.05$ , \*\* where  $p < 0.002$ ).

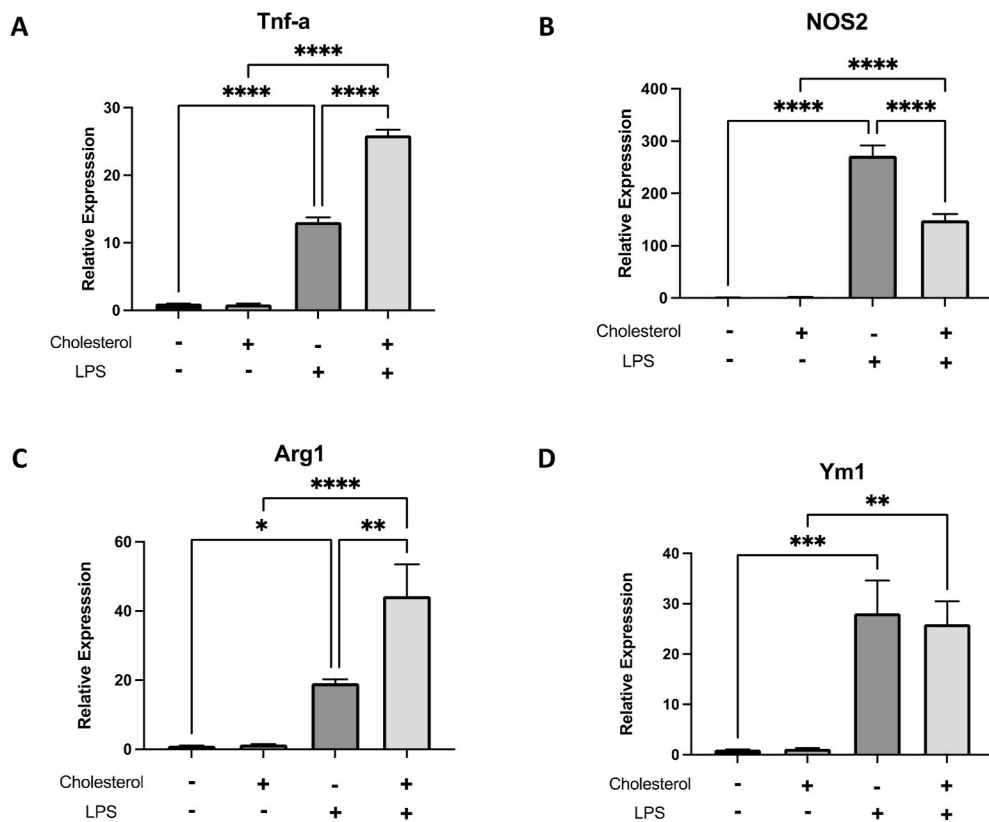


**Fig. 4. Accumulation of cholesterol altered the response to M1 and M2 stimulus.** Quantitative levels of transcriptional activation of M1 gene *TNF- $\alpha$*  (A) and another M1 marker *nos2* (B) expression were measured by qPCR in macrophages after exposure to cholesterol. (C) and (D) represents the expression level of anti-inflammatory status *Arg1* and *Ym1* genes in macrophages after cholesterol treatment. Each column represents the mean  $\pm$  standard error of at least three independent experiments. Symbols indicate a significant difference between control group and treated group (\* where  $p < 0.05$ , \*\* where  $p < 0.002$ , \*\*\* where  $p < 0.0002$ , \*\*\*\* where  $P < 0.0001$ ).

cholesterol activates inflammatory signaling, with increasing production of inflammatory mediators without inflammatory stimulation [9, 10]. The cellular responses of cholesterol laden macrophage against pro-inflammatory or anti-inflammatory stimuli have not been examined. Based on our data, the metabolic status of cholesterol-enriched macrophages suggested their immunological phenotypes to be more responsive to pro-inflammatory stimuli and more resistant to anti-inflammatory signals. The control and cholesterol-enriched macrophages were treated with TLR agonist lipopolysaccharides (LPS). The extent of transcriptional activation of M1 gene tumor necrosis factor- $\alpha$  (TNF- $\alpha$ ) increase 2.5-fold in cholesterol-loaded macrophages, while the expression of another M1 marker *nos2*, which encodes inducible nitrogen oxidase (iNOS), were downregulated (Fig. 4A and B). In parallel, the cells were also treated with M2 stimulus interleukin-4 (IL-4). Arginase1 (Arg1) and Ym1 are commonly considered as marker of this alternative activation states. Similar to the responses to M1 stimuli, cholesterol-loaded macrophage also exhibited enhanced responses to IL-4 in Arg1 expression, but no change in Ym1 expression (Fig. 4C and D). The variation of cellular responses to M1 and M2 stimuli suggested that cholesterol induced ubiquitous alterations in various signaling pathways, changing the landscape of gene expressions, and not specific limited to inflammatory or anti-inflammatory regulations.

#### 4. Discussion

Intracellular accumulations of cholesterol could lead to a series of cellular alterations in different types of cells. In addition to the involvement in atherosclerosis, cholesterol accumulation in macrophage also alters their responses to infections and might change the innate immunity phenotypes. Cholesterol is a sterol synthesized by animal cells, and also comes from the diet. The biological function of cholesterol is to maintain the integrity and fluidity of cell membranes and to serve as a precursor for the synthesis of essential organic macromolecules such as steroid hormones, bile acids, and vitamin D [26]. Due to its hydrophobic properties, cholesterol is permeable to plasma membrane and could integrate to plasma membrane and membranous organelles. The accumulation induces the alterations of the properties and functions of the organelles. Previous studies demonstrated accumulation on mitochondria causes apoptosis in various cells. Xu et al. reported concentration dependent effects of free cholesterol treatment on macrophage viability [18]. In this study we aimed to investigate the influences of accumulated cholesterol on macrophage functions. At 20  $\mu\text{g/ml}$  for 24 h of free cholesterol exposure, no obvious apoptosis can be detected. Mitochondria related apoptotic genes were not upregulated. To confirm the loading of cholesterol we used flow cytometry to verify the cell properties of treated macrophage. Alterations on both cell size the cell composition can be detected. Consistent with the observations that accumulation of cholesterol in macrophage cause the increased compartmentation-like structure, the increase of cell granulation assured the accumulation of cholesterol. Thus, the treatment conditions were chosen to generated non-apoptotic cholesterol loaded macrophages.

Unlike fatty acid, cholesterol generally is not utilized as an energy source. The excess of intracellular cholesterol does not necessarily trigger overloaded oxidative phosphorylation. The effects of cholesterol integration on mitochondria functions have only been examined in a few cell types. We evaluated the mitochondria functions by mitochondrial stress test. Although mitochondrial membranes are relatively cholesterol-poor, comparing to the other organelles, cholesterol is required for the biogenesis and membrane maintenance of mitochondria [27]. The alterations of membrane fluidity might cause the dysfunctions of electron transport chain. For example, *Srca* knockout mice exhibit increase of saturated fatty acid and decrease of polyunsaturated fatty acids which are associated with a reduction in linked complex I/III activity of the electron transport chain [28]. Additionally, cholesterol enrichment in liver mitochondria also results in the disruption of the

assembly of respiratory supercomplexes [16]. Therefore, it is possible that the reduction of ATP production implied that the integration of cholesterol to mitochondrial membrane possibly disruption the formation of electron transport complex and consequently inhibited the oxidative phosphorylation. Our results also suggested that the mitochondrial membrane properties were not affected. In addition to mitochondrial respiration, the non-mitochondria oxygen consumption was also inhibited, implying that influences of cholesterol on cellular metabolism are pleiotropic. Moreover, as the OCR was decreased, ECAR did not significantly changed. The ratio between OCR vs ECAR was decreased, meaning the metabolic stages switched toward more glycolytic by cholesterol loading in macrophages. The data suggested that accumulation of cholesterol induced metabolic reprogramming in macrophages, possibly leading to functional alterations.

Increased mitochondrial cholesterol levels and decreased membrane fluidity ameliorated 2-oxoglutarate carrier activity [17], which leads to reduced  $\alpha$ -ketoglutarate transport and impaired glutathione (GSH) import into mitochondria. As GSH is synthesized exclusively in the cytosol, the impaired GSH import into mitochondria leads to a depletion of mitochondrial GSH (mGSH) and greater sensitivity to oxidative stress-inducing agents, which is reflected in higher ROS generation by mitochondria with increased cholesterol [19]. Treatment with a membrane-permeable glutathione ethyl ester prevents cellular dysfunction and cell death in several cell models with increased mitochondrial cholesterol levels [29,30], indicating that the depletion of mGSH is a key factor in the pathological consequences of mitochondrial cholesterol accumulation. Our data revealed an opposite feature. Exposure to cholesterol decreased the generation of intracellular ROS/RNS, indicating the cellular responses to excess cholesterol varies with cell types. In macrophages, accumulation of cholesterol suppressed the generation of ROS/RNS from the major sources: oxidative phosphorylation and non-mitochondrial oxygen consumption, which mainly composed of enzyme activities such as NADPH oxidase and iNOS. The increase of uncoupling also assisted to reduce the intracellular ROS/RNS levels. In comparison, oxidized cholesterol induces increase of oxidative stress in human macrophage [31]. Our data also showed differential effects of oxidized cholesterol and free cholesterol.

Numerous evidences have pointed out that metabolic status or oxidative phosphorylation has profound impacts on macrophage functions. As mentioned previously, the decrease of oxidative phosphorylation or increase of glycolysis induces macrophage switching toward pro-inflammatory M1 status. On the other hand, it has been reported that the enhancement of oxidative stress suppresses the activity of a transcription repressor of pro-inflammatory gene expression under normoxic conditions [32]. Our data indicated that both oxidative phosphorylation and the generation of ROS/RNS were suppressed. Therefore, we furthered measured the macrophage responses to both pro-inflammatory and anti-inflammatory stimuli. The common feature of M1 genes is that they all responsible to TLR signaling and NF- $\kappa$ B activation. Also, both Arg1 and Ym1 genes are transcriptional regulated by IL-4. Our data showed the diverse effects on both M1 and M2 stimuli. Combining all the results, the integration of cholesterol induces ubiquitous changes in macrophage, not limited to the mitochondrial metabolic reprogramming or macrophage polarization. The alterations on membrane fluidity and integrity affect multiple signaling pathways. That might explain the characteristics changes of macrophages in hypercholesterolemia and other metabolic disease patients.

#### Author's contribution

Yi-Chou Chiu and Pei-Wen Chu carried out experiments and analyzed the results. Hua-Ching Lin carried out designed and discussion. Shau-Kwaun Chen conceived, designed, coordinated the study, and prepared and reviewed the manuscript. All authors read and approved the final version of the manuscript.

## Declaration of competing interest

The authors declare that they have no known competing financial interests or personal relationships that could have appeared to influence the work reported in this paper.

## Data availability

Data will be made available on request.

## Acknowledgements

This research was supported by the Cheng Hsin General Hospital, Taipei City, Taiwan (grant numbers: CHGH108, CHGH109-(N)13).

## References

- [1] A. Viola, F. Munari, R. Sanchez-Rodriguez, T. Scolaro, A. Castegna, The metabolic signature of macrophage responses, *Front. Immunol.* 10 (2019) 1462.
- [2] M.I. Stunault, G. Bories, R.R. Guinamard, S. Ivanov, Metabolism plays a key role during macrophage activation, *Mediat. Inflamm.* 2018 (2018) 2426138.
- [3] H. Zuo, Y. Wan, Metabolic reprogramming in mitochondria of myeloid cells, *Cells* (2019) 9.
- [4] E.M. Palsson-McDermott, L.A.J. O'Neill, Targeting immunometabolism as an anti-inflammatory strategy, *Cell Res.* 30 (2020) 300–314.
- [5] C. Diskin, E.M. Palsson-McDermott, Metabolic modulation in macrophage effector function, *Front. Immunol.* 9 (2018) 270.
- [6] J. Yan, T. Horng, Lipid metabolism in regulation of macrophage functions, *Trends Cell Biol.* 30 (2020) 979–989.
- [7] E. Stragliotto, M. Camera, A. Postiglione, M. Sirtori, G. Di Minno, E. Tremoli, Functionally abnormal monocytes in hypercholesterolemia, *Arterioscler. Thromb.* 13 (1993) 944–950.
- [8] A. Remmerie, C.L. Scott, Macrophages and lipid metabolism, *Cell. Immunol.* 330 (2018) 27–42.
- [9] K.J. Moore, F.J. Sheedy, E.A. Fisher, Macrophages in atherosclerosis: a dynamic balance, *Nat. Rev. Immunol.* 13 (2013) 709–721.
- [10] I. Tabas, K.E. Bornfeldt, Macrophage phenotype and function in different stages of atherosclerosis, *Circ. Res.* 118 (2016) 653–667.
- [11] T. Karasawa, M. Takahashi, The crystal-induced activation of NLRP3 inflammasomes in atherosclerosis, *Inflamm. Regen.* 37 (2017) 18.
- [12] Y. Jin, J. Fu, Novel insights into the NLRP3 inflammasome in atherosclerosis, *J. Am. Heart Assoc.* 8 (2019), e012219.
- [13] W.G. Jerome, Lysosomes, cholesterol and atherosclerosis, *Clin. Lipidol.* 5 (2010) 853–865.
- [14] V.N. Sukhorukov, V.A. Khotina, Y.S. Chegodaev, E. Ivanova, I.A. Sobenin, A. N. Orekhov, Lipid metabolism in macrophages: focus on atherosclerosis, *Biomedicines* 8 (2020).
- [15] D. Casares, P.V. Escriba, C.A. Rossello, Membrane lipid composition: effect on membrane and organelle structure, function and compartmentalization and therapeutic avenues, *Int. J. Mol. Sci.* 20 (2019).
- [16] E. Solsona-Vilarrasa, R. Fucho, S. Torres, S. Nunez, N. Nuno-Lambarri, C. Enrich, C. Garcia-Ruiz, J.C. Fernandez-Checa, Cholesterol enrichment in liver mitochondria impairs oxidative phosphorylation and disrupts the assembly of respiratory supercomplexes, *Redox Biol.* 24 (2019) 101214.
- [17] O. Coll, A. Colell, C. Garcia-Ruiz, N. Kaplowitz, J.C. Fernandez-Checa, Sensitivity of the 2-oxoglutarate carrier to alcohol intake contributes to mitochondrial glutathione depletion, *Hepatology* 38 (2003) 692–702.
- [18] X. Xu, A. Zhang, N. Li, P.L. Li, F. Zhang, Concentration-dependent diversification effects of free cholesterol loading on macrophage viability and polarization, *Cell. Physiol. Biochem.* 37 (2015) 419–431.
- [19] L.A. Martin, B.E. Kennedy, B. Karten, Mitochondrial cholesterol: mechanisms of import and effects on mitochondrial function, *J. Bioenerg. Biomembr.* 48 (2016) 137–151.
- [20] E. Ramond, A. Jamet, M. Coureuil, A. Charbit, Pivotal role of mitochondria in macrophage response to bacterial pathogens, *Front. Immunol.* 10 (2019) 2461.
- [21] C.R. LaPensee, J.E. Mann, W.E. Rainey, V. Crudo, S.W. 3rd Hunt, G.D. Hammer, ATR-101, a selective and potent inhibitor of acyl-CoA acyltransferase 1, induces apoptosis in H295R adrenocortical cells and in the adrenal cortex of dogs, *Endocrinology* 157 (2016) 1775–1788.
- [22] L.J. Berghaus, J.N. Moore, D.J. Hurley, M.L. Vandenplas, B.P. Fortes, M.A. Wolfert, G.J. Boons, Innate immune responses of primary murine macrophage-lineage cells and RAW 264.7 cells to ligands of Toll-like receptors 2, 3, and 4, *Comp. Immunol. Microbiol. Infect. Dis.* 33 (2010) 443–454.
- [23] A.I.U. Shearn, V. Deswaerte, E.L. Gautier, F. Saint-Charles, J. Pirault, L. Bouchareychas, E.B. Rucker III, S. Beliard, J. Chapman, W. Jessup, T. Huby, P. Lesnik, Bcl-x inactivation in macrophages accelerates progression of advanced atherosclerotic lesions in Apoe<sup>-/-</sup> mice, *Arterioscler. Thromb. Vasc. Biol.* 32 (2012) 1142–1149.
- [24] H. Oguro, The roles of cholesterol and its metabolites in normal and malignant hematopoiesis, *Front. Endocrinol.* 10 (2019) 204.
- [25] M. Mari, A. Morales, A. Colell, C. Garcia-Ruiz, J.C. Fernandez-Checa, Mitochondrial glutathione, a key survival antioxidant, *Antioxidants Redox Signal.* 11 (2009) 2685–2700.
- [26] R.Z. Zhao, S. Jiang, L. Zhang, Z.B. Yu, Mitochondrial electron transport chain, ROS generation and uncoupling (Review), *Int. J. Mol. Med.* 44 (2019) 3–15.
- [27] L.A. Martin, B.E. Kennedy, B. Karten, Mitochondrial cholesterol: mechanisms of import and effects on mitochondrial function, *J. Bioenerg. Biomembr.* 48 (2016) 137–151.
- [28] C.E. Ellis, E.J. Murphy, D.C. Mitchell, M.Y. Golovko, F. Scaglia, G.C. Barcelo-Coblijn, R.L. Nussbaum, Mitochondrial lipid abnormality and electron transport chain impairment in mice lacking  $\alpha$ -synuclein, 25, 2005, pp. 10190–10201.
- [29] F. Villarroya, M. Peyrou, M. Giral, Transcriptional regulation of the uncoupling protein-1 gene, *Biochimie* 134 (2017) 86–92.
- [30] M. Mari, E. de Gregorio, C. de Dios, V. Roca-Agujetas, B. Cucarull, A. Tutusaus, A. Morales, A. Colell, Mitochondrial glutathione: recent insights and role in disease, *Antioxidants* 9 (2020).
- [31] O.J. Lara-Guzman, A. Gil-Izquierdo, S. Medina, E. Osorio, R. Alvarez-Quintero, N. Zuluaga, C. Oger, J. Galano, T. Durand, K. Munoz-Durango, Oxidized LDL triggers changes in oxidative stress and inflammatory biomarkers in human macrophages, *Redox Biol.* 15 (2018) 1–11.
- [32] Y. Morel, R. Barouki, Repression of gene expression by oxidative stress, *Biochem. J.* 342 Pt 3 (1999) 481–496.